СТРОИТЕЛЬНАЯ МЕХАНИКА ИНЖЕНЕРНЫХ КОНСТРУКЦИЙ И СООРУЖЕНИЙ
STRUCTURAL MECHANICS OF ENGINEERING CONSTRUCTIONS AND BUILDINGS

2026. 22(2). 93–104

ISSN 1815-5235 (Print), 2587-8700 (Online)
HTTP://JOURNALS.RUDN.RU/STRUCTURAL-MECHANICS

АНАЛИТИЧЕСКИЕ И ЧИСЛЕННЫЕ МЕТОДЫ РАСЧЕТА КОНСТРУКЦИЙ
ANALYTICAL AND NUMERICAL METHODS OF STRUCTURAL ANALYSIS

DOI: 10.22363/1815-5235-2026-22-2-93-104
EDN: JZQSKW

Research article / Научная статья

Prediction of Thermal Stress in Hardening Mass Concrete Structures Using Temperature Monitoring Data

Vasilina S. Tyurina, Anton S. Chepurnenko✉, Batyr M. Yazyev

Don State Technical University, *Rostov-on-Don, Russian Federation*
✉ anton_chepurnenk@mail.ru

Received: January 30, 2026
Revised: March 13, 2026
Accepted: March 20, 2026

Abstract. Thermal stress during the hardening of mass concrete structures is a significant risk factor for early cracking, which directly impacts the durability and load-bearing capacity of buildings and structures. Simplified calculation methods based on hypotheses about the pattern of temperature and stress distributions often demonstrate low accuracy, necessitating the search for more advanced approaches to stress state prediction. This paper proposes a method for predicting the thermal stress in mass concrete foundation slabs based on artificial neural networks (ANNs) using real-time temperature monitoring data. Three ANN architectures were investigated: recurrent, feedforward, and cascade. A comprehensive dataset, including 499,800 records obtained from parametric finite element calculations, was compiled for training. The models demonstrated high prediction accuracy, with the feedforward neural network achieving the best result, with a mean-square error of 0.025 MPa². Verification using experimental data confirmed the practical applicability of the approach, including the ability to predict the timing of crack formation. The developed method enables efficient and less computationally expensive analysis of temperature monitoring data in real time compared to traditional modeling, thereby improving the reliability of building structures.

Keywords: mass concrete structures, foundation slab, thermal stresses, machine learning, monitoring, early crack formation

Authors' contribution: *Tyurina V.S.* — investigation, data processing, graphic design, text writing; *Chepurnenko A.S.* — software, text draft, review and editing; *Yazyev B.M.* — supervision, conceptualization. The authors read and approved the final version of the article.

Conflicts of interest. The authors declare that there is no conflict of interest.

A statement about data availability. The training dataset is available for download at: https://doi.org/10.13140/RG.2.2.33439.62880/

Funding. The study was supported by the grant of the Russian Science Foundation No. 25-19-00164, https://rscf.ru/project/25-19-00164/

For citation: Tyurina VS, Chepurnenko AS, Yazyev BM. Prediction of thermal stress in hardening mass concrete structures using temperature monitoring data. *Structural Mechanics of Engineering Constructions and Buildings.* 2026;22(2):93–104. http://doi.org/10.22363/1815-5235-2026-22-2-93-104 EDN: JZQSKW

Vasilina S. Tyurina, Candidate of Technical Sciences, Associate Professor of the Department of Structural Mechanics and Theory of Structures, Don State Technical University, 1 Gagarin Sq., Rostov-on-Don, 344003, Russian Federation; eLIBRARY SPIN-code: 8808-2687, ORCID: 0009-0001-6399-401X; e-mail: vasilina.93@mail.ru

Anton S. Chepurnenko, Doctor of Technical Sciences, Professor of the Department of Structural Mechanics and Theory of Structures, Don State Technical University, 1 Gagarin Sq., Rostov-on-Don, 344003, Russian Federation; eLIBRARY SPIN-code: 7149-7981, ORCID: 0000-0002-9133-8546; e-mail: anton_chepurnenk@mail.ru

Batyr M. Yazyev, Doctor of Technical Sciences, Professor of the Department of Structural Mechanics and Theory of Structures, Don State Technical University, 1 Gagarin Sq., Rostov-on-Don, 344003, Russian Federation; eLIBRARY SPIN-code: 5970-5350, ORCID: 0000-0002-5205-1446; e-mail: ps62@yandex.ru

Прогнозирование температурных напряжений в твердеющих массивных монолитных конструкциях по данным мониторинга температур

В.С. Тюрина, А.С. Чепурненко✉, Б.М. Язьев

Донской государственный технический университет, *Ростов-на-Дону, Российская Федерация*
✉ anton_chepurnenk@mail.ru

Поступила в редакцию: 30 января 2026 г.
Доработана: 13 марта 2026 г.
Принята к публикации: 20 марта 2026 г.

Аннотация. Температурные напряжения в процессе твердения массивных монолитных конструкций являются значимым фактором риска раннего трещинообразования, что напрямую влияет на долговечность и несущую способность зданий и сооружений. Упрощенные методы расчета, основанные на гипотезах о характере распределения температур и напряжений, часто демонстрируют невысокую точность, что актуализирует поиск более совершенных подходов к прогнозированию напряжённого состояния. Авторами предложен метод прогнозирования температурных напряжений в массивных монолитных фундаментных плитах на основе искусственных нейронных сетей (ИНС) с использованием данных мониторинга температур в режиме реального времени. Для этого были исследованы три архитектуры ИНС — рекуррентная, прямого распространения и каскадная. В целях обучения сформирован обширный датасет, включающий 499 800 записей, полученных на основе параметрических конечно-элементных расчётов. Модели продемонстрировали высокую точность предсказания, при этом наилучший результат показала нейросеть прямого распространения со среднеквадратической ошибкой 0,025 МПа². Верификация на экспериментальных данных подтвердила практическую применимость подхода, включая способность прогнозировать момент образования трещин. Разработанный метод позволяет эффективно и с меньшими вычислительными затратами, по сравнению с традиционным моделированием, анализировать данные мониторинга температур в реальном времени, что способствует повышению надёжности строительных конструкций.

Ключевые слова: массивные монолитные конструкции, фундаментная плита, температурные напряжения, машинное обучение, мониторинг, ранее трещинообразование

Вклад авторов: *Тюрина В.С.* — проведение исследования, обработка данных, графическое оформление, написание текста; *Чепурненко А.С.* — программное обеспечение, подготовка текста статьи, рецензирование и редактирование; *Язьев Б.М.* — общее научное руководство, формулировка концепции исследования. Авторы ознакомлены с окончательной версией статьи и одобрили ее.

Заявление о конфликте интересов. Авторы заявляют об отсутствии конфликта интересов.

Заявление о доступности данных. Обучающий датасет доступен для скачивания по ссылке: https://doi.org/10.13140/RG.2.2.33439.62880

Финансирование. Исследование выполнено за счет гранта Российского научного фонда № 25-19-00164, https://rscf.ru/project/25-19-00164/

Для цитирования: *Тюрина В.С., Чепурненко А.С., Язьев Б.М.* Прогнозирование температурных напряжений в твердеющих массивных конструкциях по данным мониторинга температур // Строительная механика инженерных конструкций и сооружений. 2026. Т. 22. № 2. С. 93–104. http://doi.org/10.22363/1815-5235-2026-22-2-93-104 EDN: JZQSKW

1. Introduction

A widespread problem for mass concrete and reinforced concrete structures is the formation of temperature cracks during the early stages of hardening. During cement hydration, a large amount of heat is released, causing uneven temperature rise: the core of the structure develops much more heat than the surface. During subsequent cooling, tensile stress that exceeds the strength of early age concrete arises, leading to cracking [1; 2]. This reduces the strength, durability, and aesthetics of structures and increases the risk of corrosion [3].

The most common tool for assessing the risk of early cracking is finite element modeling. It allows to analyse the evolution of temperature distributions and stresses, taking into account changes in the key properties of concrete over time. It is critical to account for the dependence of concrete strength and deformation characteristics on time and hardening conditions, since ignoring this factor leads to an incorrect evaluation of the stress state [4–6].

A limitation of finite element modeling is the inability to account for uncertainties in input data, including ambient and foundation temperatures, wind speed, variations in concrete heat release when using

cements from different manufacturers, etc. Variability in input data can lead to significant deviations of the actual temperature and stress values in the structure from the expected. In existing monitoring systems for mass structures (Maturix[1], Giatec SmartRock[2]), only temperature measurements are typically taken, not stress [7]. Stress can be determined indirectly from strain; however, sensors for measuring strain are highly complex and expensive, as they must be capable of compensating their readings with respect to temperature [8]. Therefore, the problem of quickly assessing the actual stress in the structure based on real-time temperature monitoring data is of great relevance. Such an assessment allows for timely measures to be taken to prevent early cracking, including additional thermal insulation of surfaces to reduce temperature gradients when the stress approaches a dangerous level [9].

In [10], a simplified method for estimating thermal stress in mass concrete foundation slabs was proposed. Instead of the traditional approach based on the temperature difference between the center and the surface [11–14], the proposed method uses temperature data at three characteristic points along the slab thickness (bottom, middle, and top). The formulas were verified using numerical simulation and demonstrated high accuracy for slabs up to 2 meters thick. Significant errors for slab thickness values of 2 meters and greater are associated with the assumption of a parabolic distribution of temperature and stress along the slab thickness. This article aims to overcome this limitation using machine learning methods. It should be noted that previously, machine learning methods were used only to predict the heat release of concrete [15], its thermal conductivity coefficient [16], and strength characteristics [17–18], estimating the temperature difference between the center and the surface of the structure [19], determining the maximum stress level for fixed input data [20], and designing an optimal concrete mix composition [21–24].

Unlike previous studies, the aim of this article is to develop and validate a method for predicting thermal stress in mass concrete foundation slabs based on limited temperature monitoring data collected at characteristic points along the slab thickness, using artificial neural networks. To achieve this objective, the following tasks were addressed:

1. Create a representative training dataset based on parametric finite element calculations, covering variations in geometric, strength, and thermophysical parameters.
2. Develop and train three artificial neural network architectures (recurrent, feedforward, and cascade) for stress prediction based on temperature monitoring data.
3. Evaluate the accuracy and comparative performance of the proposed models based on training quality metrics and regression curve analysis.
4. Verify the developed models using experimental data for a real foundation slab.

2. Methods

MATLAB R2021a (Neural Network Toolbox) serves as the environment for implementing machine learning models. Seven variables were selected as input parameters for the machine learning models: temperatures at three points along the slab thickness (T_{bot} at the bottom surface, T_{mid} in the middle of the slab, and T_{up} at the top surface), time t in days, concrete compressive strength class B according to the Russian Federal Standard GOST 18105-2018[3], slab thickness h, and hardening rate (*rate*). The output parameters of the models are three values: stress σ_{bot} at the bottom surface, σ_{mid} in the middle surface, and σ_{up} at the top surface (MPa). Three artificial neural network (ANN) architectures are considered:

1. Layer recurrent neural network (Figure 1);
2. Feedforward neural network (Figure 2);
3. Cascade forward neural network (Figure 3).

[1] Maturix — Concrete temperature, strength and maturity monitoring. Available from: https://maturix.com/ (accessed: 27.01.2026).

[2] Giatec Scientific Inc — Smart Construction Testing Technologies. Available from: https://www.giatecscientific.com/ (accessed: 27.01.2026).

[3] GOST 18105-2018. Concretes. Rules for control and assessment of strength. 2019. Available from: https://www.mos.ru/upload/documents/files/2071/GOST18105-2018.pdf (accessed: 27.01.2026)

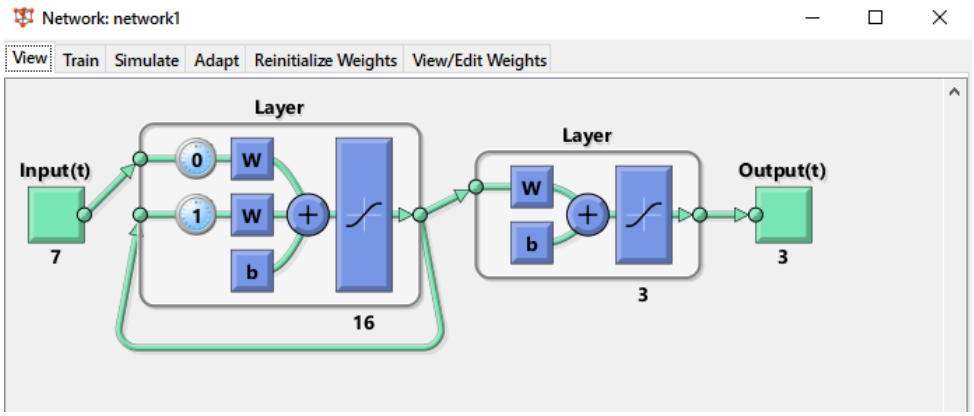

Figure 1. Recurrent neural network (screenshot from MATLAB)

S o u r c e: made by V.S. Tyurina.

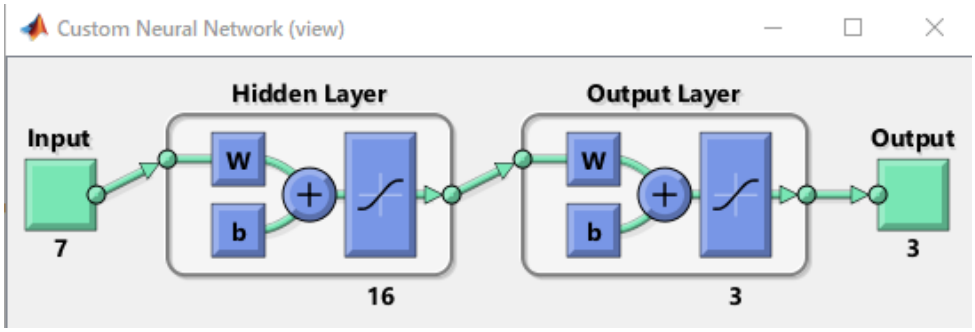

Figure 2. Feedforward neural network (screenshot from MATLAB)

S o u r c e: made by V.S. Tyurina.

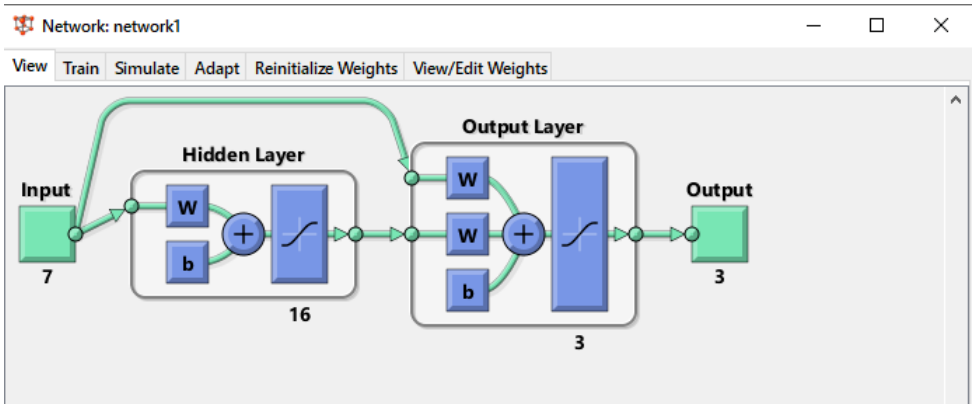

Figure 3. Cascade forward neural network (screenshot from MATLAB**)**

S o u r c e: made by V.S. Tyurina.

For all ANN architectures, a single hidden layer with sixteen neurons was used. When forming the training dataset, the slab thickness varied from 1 to 3 m in 0.5 m increments, the heat transfer coefficient on the upper surface ranged from 2 to 30 W/(m^2·°C) in 4 W/(m^2·°C) increments, and the concrete class ranged from B25 to B45 in 5 MPa increments. The ambient temperature varied from 5 to 35 °C in 5 °C increments. Three integer values were introduced for the hardening rate: 1, 2, and 3, corresponding to high-early-strength, regular, and low-early-strength concrete. The selected ranges of input parameter variations cover the most common parameters for concrete placement and the geometry of mass concrete foundation slabs.

The heat release function was defined by equation [25]:

$$Q(t) = Q_{28} \exp\left(k \left(1 - \left(\frac{28}{t-b} \right)^x \right) \right), \quad (1)$$

where Q_{28} is the total heat release per 1 m^3 of concrete at 28 days, k and x are coefficients determining the kinetics of heat release, and b is the induction period.

The heat release parameters are listed in Table 1.

For each set of values [B h h_{up} T_∞ *rate*], the temperature distribution and stress state were calculated, with temperature and stress values determined at three characteristic points (bottom, middle, top) for 119 time points ranging from 0.5 to 30 days, with a step size of 0.25 days. The temperature distribution was calculated using the finite element method (FEM) in a simplified one-dimensional formulation according to the method described in [26]. The stress state was calculated using the method presented in [27].

Table 1. **Parameters in the heat release equation**

Parameter	k	x	Q_{28}, MJ/m^3	b, days
High-early-strength (1)	0.14	0.4	$130 + 3\cdot(B - 25)$	0.167
Regular (2)	0.19	0.51		
Low-early-strength (3)	0.24	0.62		

S o u r c e: made by V.S. Tyurina.

The thermophysical properties of the soil were assumed to be constant and equal to: thermal conductivity coefficient $\lambda_g = 0.9$ W/(m·°C), specific heat capacity $c_g = 750$ *J*/(kg·°C), and density $\rho_g = 1800$ kg/m³. The following values of thermophysical properties of concrete were assumed: $\lambda = 2.67$ W/(m·°C), $c = 1000$ *J*/(kg·°C), $\rho = 2400$ kg/m³. The function describing the change in concrete compressive strength was defined by equation [28]:

$$R = R_{28} \exp\left(s \left(1 - \sqrt{\frac{28}{t_{eq} - b}} \right) \right), \quad (2)$$

where $R_{28} = B + 12$ is the compressive strength of concrete at 28 days, s is a coefficient dependent on the hardening kinetics of concrete, $t_{eq} = DM / 20$ is the equivalent age of concrete, expressed in terms of its degree of maturity DM:

$$DM = \int_0^t T(\tau) d\tau, \quad (3)$$

where $T(\tau)$ is the temperature at a point at age τ.

Coefficient s was taken to be 0.2 for high-early-strength concrete, 0.35 for regular concrete, and 0.5 for low-early-strength concrete. The modulus of elasticity of concrete was determined as a function of compressive strength using formula [28]:

$$E(R) = 22265 \left(\frac{R}{10} \right)^{0.28}, \text{ MPa}. \quad (4)$$

The value of R in Equation (4) should be substituted in MPa. Poisson's ratio of concrete was assumed to be independent of time and hardening temperature ($\nu = 0.2$). Up to an equivalent age of 12 hours, the modulus of elasticity of concrete was assumed to be zero (it was assumed that the concrete was not yet a solid and contained no stress). The layering of the concrete mix was not taken into account in the calculation. The initial soil temperature was assumed to be equal to the ambient temperature.

The calculated temperature values T_{bot}, T_{mid}, T_{up} were placed in the input parameter array along with the values [B, h, rate] and time t. Stress values σ_{bot}, σ_{mid}, σ_{up} were placed in the target values array of the output variables. The total volume of the training dataset consisted of 4200 numerical experiments (4200 × 119 = 499800 rows). A sample of the generated training dataset is presented in Table 2.

Table 2. **A fragment of the training dataset**

No.	Input parameters							Output parameters		
	T_{bot}, °C	T_{mid}, °C	T_{up}, °C	t, days	B, MPa	h, m	rate	σ_{bot}, MPa	σ_{mid}, MPa	σ_{up}, MPa
1	23.97	31.98	29.18	0.5	25	1	1	0.000	0.000	0.000
2	27.31	35.90	32.27	0.75	25	1	1	–0.002	–0.088	0.094
3	29.31	37.68	33.69	1	25	1	1	–0.095	–0.116	0.178
4	30.67	38.54	34.33	1.25	25	1	1	–0.248	–0.108	0.256
5	31.63	38.91	34.53	1.5	25	1	1	–0.424	–0.087	0.335
6	32.33	39.01	34.46	1.75	25	1	1	–0.606	–0.062	0.415
7	32.84	38.93	34.24	2	25	1	1	–0.784	–0.036	0.492
8	33.20	38.73	33.91	2.25	25	1	1	–0.954	–0.010	0.565
9	33.44	38.46	33.52	2.5	25	1	1	–1.114	0.014	0.631
10	33.58	38.14	33.10	2.75	25	1	1	–1.262	0.037	0.691
11	33.66	37.77	32.65	3	25	1	1	–1.399	0.059	0.743
12	33.67	37.39	32.20	3.25	25	1	1	–1.525	0.080	0.789
13	33.62	36.98	31.74	3.5	25	1	1	–1.640	0.100	0.828
14	33.54	36.56	31.28	3.75	25	1	1	–1.745	0.118	0.861
15	33.42	36.14	30.83	4	25	1	1	–1.842	0.136	0.889
…	…	…	…	…	…	…	…	…	…	…
499786	76.22	70.58	37.56	26.5	45	3	3	–5.600	–1.337	8.696
499787	76.08	70.38	37.54	26.75	45	3	3	–5.609	–1.317	8.631
499788	75.94	70.18	37.52	27	45	3	3	–5.617	–1.297	8.566
499789	75.80	69.99	37.50	27.25	45	3	3	–5.624	–1.278	8.501
499790	75.66	69.79	37.49	27.5	45	3	3	–5.630	–1.258	8.436
499791	75.51	69.60	37.47	27.75	45	3	3	–5.636	–1.239	8.372
499792	75.37	69.41	37.45	28	45	3	3	–5.642	–1.220	8.307
499793	75.23	69.22	37.44	28.25	45	3	3	–5.647	–1.202	8.243
499794	75.09	69.03	37.42	28.5	45	3	3	–5.651	–1.184	8.179
499795	74.94	68.84	37.40	28.75	45	3	3	–5.654	–1.166	8.116
499796	74.80	68.65	37.39	29	45	3	3	–5.657	–1.148	8.053
499797	74.65	68.46	37.37	29.25	45	3	3	–5.660	–1.130	7.990
499798	74.51	68.28	37.36	29.5	45	3	3	–5.662	–1.113	7.927
499799	74.37	68.10	37.34	29.75	45	3	3	–5.663	–1.095	7.864
499800	74.22	67.91	37.32	30	45	3	3	–5.664	–1.078	7.802

S o u r c e: made by V.S. Tyurina.

The artificial neural network models were trained using the Levenberg — Marquardt algorithm. The training dataset was randomly divided into three parts: “Training,” “Validation” and “Test,” which were used for training, validation, and testing, respectively. The split ratio was 75:15:15%. The mean squared error (MSE) was used as the training quality metric:

$$MSE = \frac{1}{n}\sum_{j=1}^{n}(T_i - Y_i)^2, \tag{5}$$

where n is the training sample size, Y_i are the stress values predicted by the neural network, T_i are the target stress values.

3. Results and Discussion

The statistical characteristics of the generated dataset are presented in Table 3. The model operates reliably only within the ranges between min and max for the input parameters, since using artificial neural networks for extrapolation can lead to unpredictable results.

Table 3. **Statistical characteristics of the training dataset**

Characteristic	Input variables							Output variables		
	T_{bot}	T_{mid}	T_{up}	t	B	h	rate	σ_{bot}	σ_{mid}	σ_{up}
mean	46.35	46.16	27.78	15.25	35	2	2	–2.98	–0.52	2.42
std. dev.	15.08	16.77	12.71	8.59	7.07	0.71	0.82	2.10	0.97	3.36
min	6.21	6.32	5.23	0.50	25	1	1	–9.21	–4.53	–9.95
25%	35.96	34.20	17.64	7.75	30	1.5	1	–4.41	–1.12	0.27
50%	46.57	45.92	27.39	15.25	35	2	2	–2.94	–0.39	2.45
75%	57.40	58.05	36.59	22.75	40	2.5	3	–1.51	0.18	4.71
max	85.57	99.69	79.89	30.00	45	3	3	3.11	2.27	12.55

S o u r c e: made by V.S. Tyurina.

The correlation coefficient matrix is shown in Table 4. Table 4 indicates that a very strong positive correlation (correlation coefficient R_{XY} greater than 0.9) is observed between parameters T_{bot} and T_{mid}. A strong positive correlation ($0.7 \le R_{XY} < 0.9$) is also observed between parameters T_{up} and T_{bot}, σ_{up} and T_{bot}, σ_{mid} and T_{bot}, σ_{mid} and T_{mid}. Correlation between the temperatures at the bottom surface, in the middle of the slab, and at the top surface is explained by the fact that the heating of the structure due to hydration is accompanied by the rise in temperature at all points. Strong correlation between the temperature and stress parameters also fully corresponds to the physics of the process.

A strong negative correlation is observed between parameters σ_{up} and σ_{mid}. This is consistent with the results of [29], where it was shown that, assuming a parabolic temperature distribution along the thickness and symmetric heat transfer conditions, the following relationship holds between the increments of stresses σ_{up} and σ_{mid}:

$$2\Delta\sigma_{mid} = -\Delta\sigma_{up}. \quad (6)$$

Under asymmetric heat exchange conditions (heat exchange with the ground and the atmosphere), this relationship is disrupted, but a strong negative correlation between σ_{up} and σ_{mid} persists.

Moderate positive correlation ($0.5 \le R_{XY} < 0.7$) is observed between parameters h and T_{bot}, h and T_{mid}, h and σ_{up}. It is evident that as the slab thickness increases, the maximum temperature at the center of the structure also increases. Since most of the heat is dissipated through the top surface of the slab, the temperature at the bottom surface also increases as the thickness increases.

Moderate positive correlation ($0.3 \le R_{XY} < 0.49$) is observed between parameters T_{up} and σ_{up}, t and σ_{mid}, the hardening rate and the value of σ_{bot}. Parameters h and t, B and t, in the training dataset are completely independent.

The training process for the recurrent neural network, feedforward neural network, and cascade neural network is shown in Figures 4–6, respectively. The training process was limited to 1000 iterations. The best mean square error value at the 1000th iteration was achieved for the feedforward neural network and amounted to 0.025 MPa².

Figures 7–9 show the regression plots for the three machine learning models. The x-axis plots the target stress values T, and the y-axis plots the values Y predicted by the neural networks. The shape of the graphs for the models under consideration is similar; all points lie a short distance from the line $Y = T$. The correlation coefficients between the target and predicted values are close to one.

Table 4. **Correlation coefficient matrix**

Parameter	T_{bot}	T_{mid}	T_{up}	t	B	h	$rate$	σ_{bot}	σ_{mid}	σ_{up}
T_{bot}	1.00	0.96	0.73	–0.18	0.23	0.53	–0.06	–0.21	–0.72	0.79
T_{mid}	0.96	1.00	0.76	–0.36	0.21	0.55	–0.04	0.02	–0.83	0.84
T_{up}	0.73	0.76	1.00	–0.20	0.08	0.10	–0.01	0.26	–0.36	0.44
t	–0.18	–0.36	–0.20	1.00	0.00	0.00	0.00	–0.46	0.48	–0.34
B	0.23	0.21	0.08	0.00	1.00	0.00	0.00	–0.25	–0.11	0.15
h	0.53	0.55	0.10	0.00	0.00	1.00	0.00	–0.24	–0.68	0.63
$rate$	–0.06	–0.04	–0.01	0.00	0.00	0.00	1.00	0.47	–0.09	0.26
σ_{bot}	–0.21	0.02	0.26	–0.46	–0.25	–0.24	0.47	1.00	–0.10	0.02
σ_{mid}	–0.72	–0.83	–0.36	0.48	–0.11	–0.68	–0.09	–0.10	1.00	–0.91
σ_{up}	0.79	0.84	0.44	–0.34	0.15	0.63	0.26	0.02	–0.91	1.00

S o u r c e: made by V.S. Tyurina.

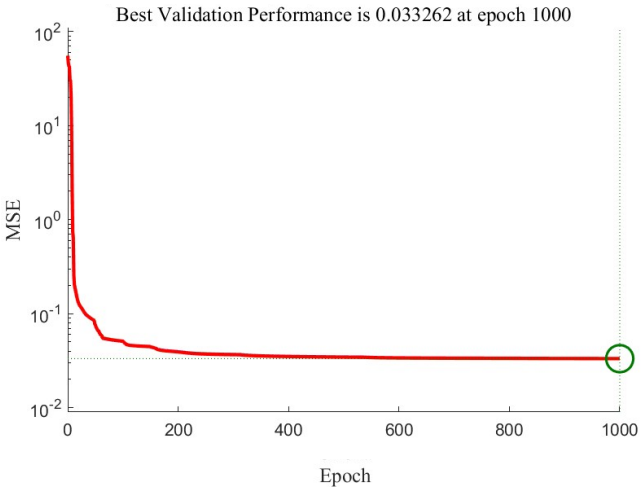

Figure 4. The training process for the recurrent neural network.
S o u r c e: made by V.S. Tyurina.

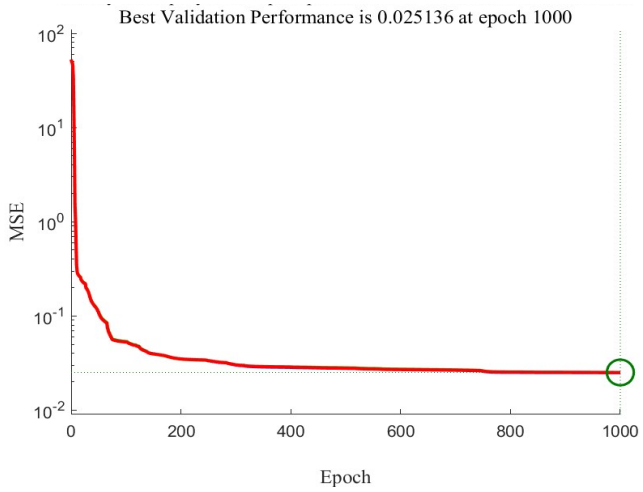

Figure 5. The training process for the feedforward neural network
S o u r c e: made by V.S. Tyurina.

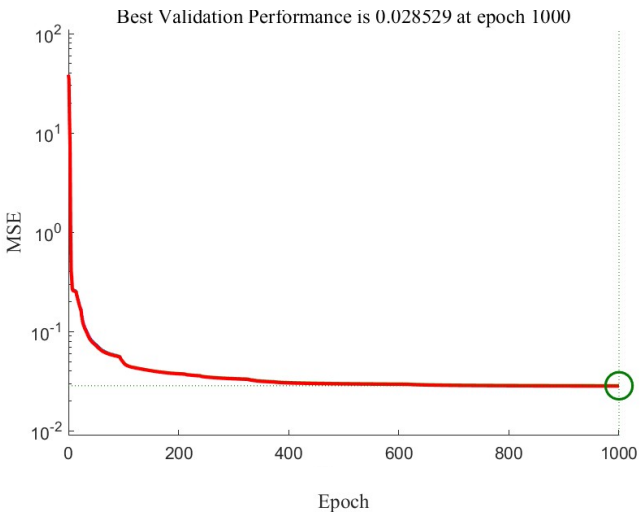

Figure 6. The training process for the cascade neural network.
S o u r c e: made by V.S. Tyurina.

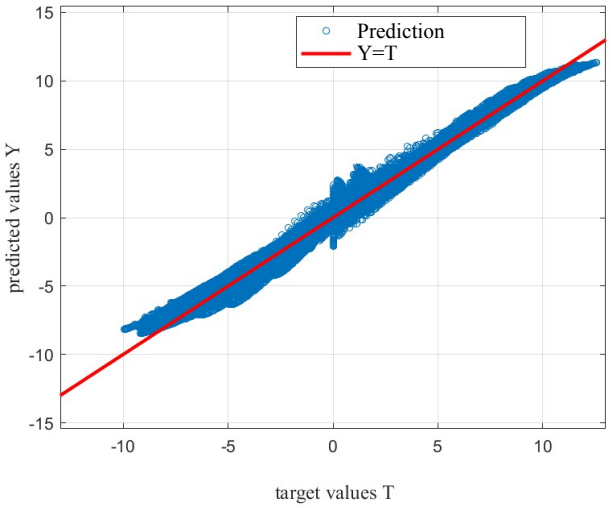

Figure 7. Regression plot for the recurrent neural network
S o u r c e: made by V.S. Tyurina.

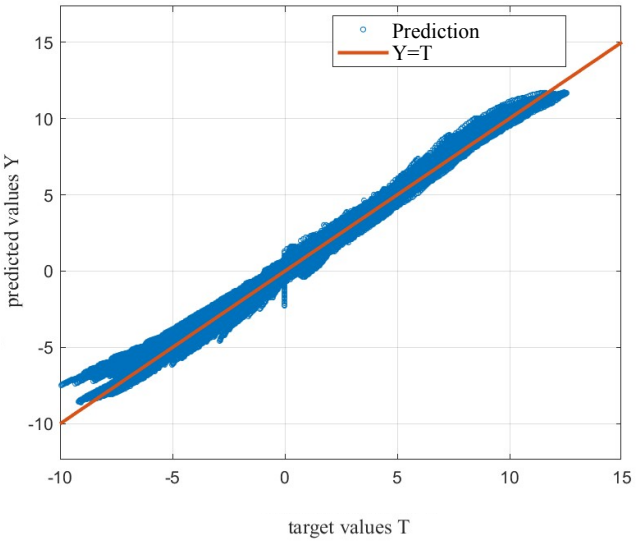

Figure 8. Regression plot for the feedforward neural network

S o u r c e: made by V.S. Tyurina.

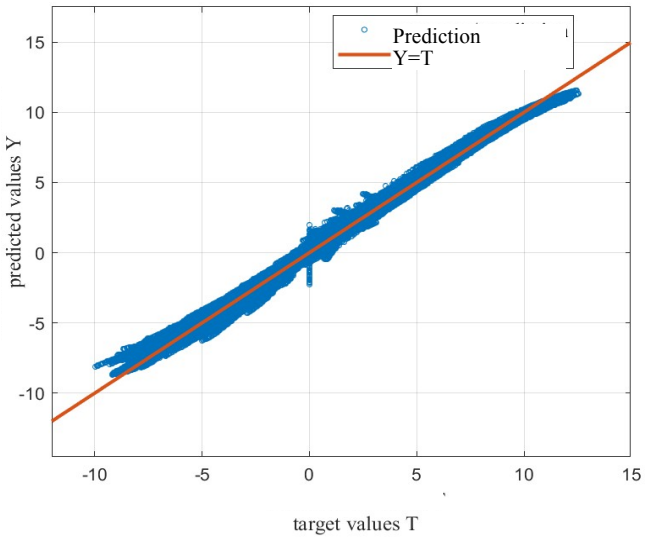

Figure 9. Regression plot for the cascade neural network

S o u r c e: made by V.S. Tyurina.

The trained models were also validated using experimental data for a mass concrete foundation slab 2 m thick, as reported in [30]. Stress predictions were performed based on experimental temperature values. The prediction results were then compared with the field measurements. Since the temperature on the top surface exhibited significant daily fluctuations, preliminary smoothing of the experimental data was applied (Figure 10). For the bottom surface and the middle of the slab, the experimental temperature values are given in Table 5.

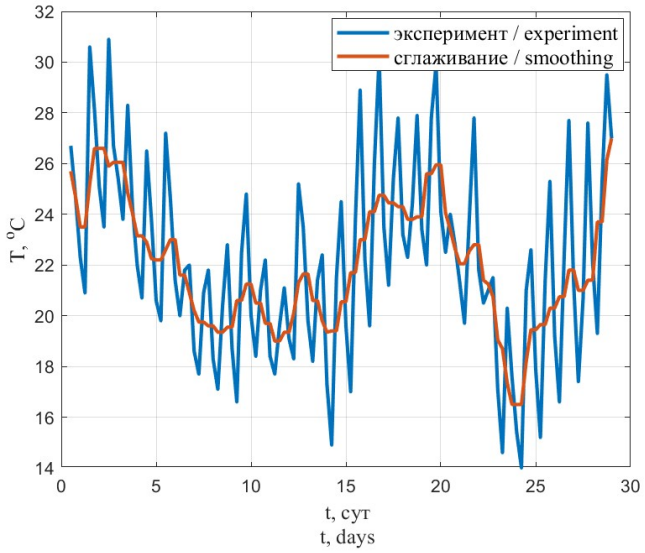

Figure 10. Graph of temperature changeon the upper surface of the slab before and after smoothing

S o u r c e: made by V.S. Tyurina.

According to the classification used in this study, the concrete used in the slab is a high-early-strength concrete with a strength class of approximately B22.5. Figure 11 shows a comparison of the predictions made by the artificial neural networks with experimental data for the center of the foundation slab. For comparison, the results of finite element modeling using relationships (2)–(4) are also presented. The heat release function in the finite element calculation was selected to ensure the best possible agreement between the calculated and experimental temperatures.

Table 5. **Experimental temperature values in the middle of the thickness and at the lower surface**

t, days	0.5	1	2	3	4	5	6	7	8	9	10	11	12	13	14
T_{mid}, °C	23.1	28.8	41.8	44.3	42.6	40	37.3	35.3	33.3	31.5	30.2	29.2	28.3	27.4	26.9
T_{bot}, °C	23	25.7	32	35	36.3	36.4	35.9	35.1	34.2	33.3	32.4	31.5	30.7	29.9	29.2

t, days	15	16	17	18	19	20	21	22	23	24	25	26	27	28	29
T_{mid}, °C	26.1	25.8	25.7	25.8	25.9	25.8	25.7	25.5	25.3	24.4	23.5	23.1	23	23	23.1
T_{bot}, °C	28.6	28.1	27.6	27.2	26.8	26.6	26.3	26.1	26	25.7	25.4	25.1	24.7	24.4	24.2

S o u r c e: made by V.S. Tyurina.

The graphs show that the three machine learning models and the FEM produce roughly the same results, with the exception of the initial time point. The feedforward neural network provides a more accurate prediction at the initial time point, exhibiting the lowest mean square error among all the models considered. At the 16-day mark during the experiment, a crack was observed in the slab, corresponding to a spike in the experimental graph. At this point in time, the neural networks predict the tensile stress value with sufficient accuracy. Deviations of the experimental results from the finite element analysis and the neural network predictions are observed in the time interval from 3 to 11 days. These can be explained by deviation of the actual time-dependent elastic modulus of concrete from that assumed in the model.

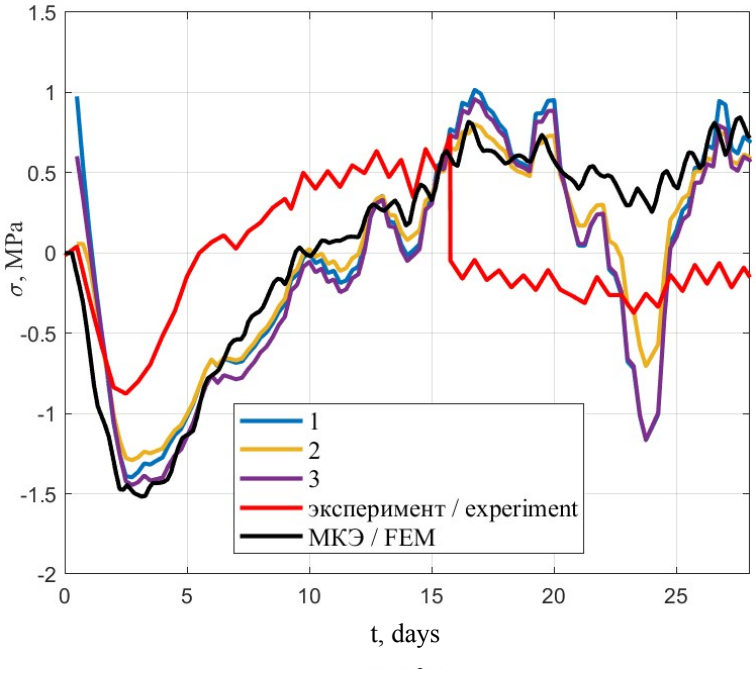

Figure 11. Comparison of neural network predictions with experimental data and finite element analysis results:
1 — recurrent neural network; *2* — feedforward neural network; *3* — cascade neural network
S o u r c e: made by V.S. Tyurina.

4. Conclusion

As part of this study, an approach for predicting thermal stress in mass concrete foundation slabs based on temperature monitoring data using machine learning methods was developed and validated. Three artificial neural network architectures were considered as models: a recurrent neural network, a feedforward neural network, and a cascade neural network. Training was conducted using a dataset of 499,800 rows, generated from 4200 numerical experiments and covering a wide range of variations in geometric, strength, and thermophysical parameters.

The feedforward neural network model yielded the best results, achieving a mean square error in the stress prediction of 0.025 MPa². All three models demonstrated high prediction accuracy, as confirmed by regression plots with correlation coefficients between the target and predicted values close to one. Verification of the developed ANN models using experimental data for a 2-m-thick slab demonstrated their adequacy and practical applicability. With particular accuracy, the models predicted the emergence of tensile stress corresponding to the crack formation observed in the experiment on the 16th day.

The proposed approach overcomes the limitations of existing methods based on the assumption of a parabolic distribution of temperature and stress, and provides accurate predictions for structures thicker than 2 m. The use of ANN significantly reduces computational costs compared to direct finite element modeling, making the method an effective tool for quick analysis of monitoring data in real-time.

Thus, the application of machine learning methods to predict thermal stress in hardening mass concrete structures is a promising area of research that helps to improve the accuracy of stress state evaluation and prevent early cracking.

References

1. Safiuddin M, Kaish ABM, Woon C-O, Raman SN. Early-age cracking in concrete: causes, consequences, remedial measures, and recommendations. *Applied Sciences.* 2018;8(10):1730. https://doi.org/10.3390/app8101730.

2. Klemczak B, Batog M, Pilch M, Żmij A. Analysis of cracking risk in early age mass concrete with different aggregate types. *Procedia engineering.* 2017;193:234–241. https://doi.org/10.1016/j.proeng.2017.06.209

3. Mazzoli A, Monosi S, Plescia ES. Evaluation of the early-age-shrinkage of fiber reinforced concrete (FRC) using image analysis methods. *Construction and Building Materials.* 2015;101:596–601. https://doi.org/10.1016/j.conbuildmat.2015.10.090

4. Waller V, d'Aloïa L, Cussigh F, Lecrux S. Using the maturity method in concrete cracking control at early ages. *Cement and Concrete Composites.* 2004;26(5):589–599. https://doi.org/10.1016/S0958-9465(03)00080-5

5. Alos Shepherd D, Dehn F. Experimental study into the mechanical properties of plastic concrete: Compressive strength development over time, tensile strength and elastic modulus. *Case Studies in Construction Materials.* 2023;19:e02521. https://doi.org/10.1016/j.cscm.2023.e02521 EDN: DAARVN

6. Xu J, Shen Z, Yang S, Xie X, Yang Z. Finite element simulation of prevention thermal cracking in mass concrete. *International Journal of Computing Science and Mathematics.* 2019;10(4):327–339. https://doi.org/10.1504/IJCSM.2019.102691

7. Julia R, Agrela F, Rosales M, López-Alonso M, Cuenca-Moyano G. Execution of large-scale sustainable pavement with recycled materials and eco-hybrid additions to cement. Assessment of Mechanical Behaviour and Life Cycle. *Construction and Building Materials*. 2025;453:139558. https://doi.org/10.1016/j.conbuildmat.2025.139967 EDN: GOCOWJ

8. Namatēvs I, Gaigals G, Ozols K. ConMonity: An IoT-Enabled LoRa/LTE-M platform for multimodal, real-time monitoring of concrete curing in construction environments. *Sensors.* 2026;26:14. https://doi.org/10.3390/s26010014 EDN: CNKAJT

9. Aniskin NA, Chuc NT, Khanh PK. The use of surface thermal insulation to regulate the temperature regime of a mass concrete during construction. *Power Technology and Engineering.* 2021;55(1):1–7. https://doi.org/10.1007/s10749-021-01310-6 EDN: TSLLPN

10. Tyurina V, Chepurnenko A, Tkachev D. A simplified method for assessing thermal stresses during the construction of massive monolithic foundation slabs based on temperatures at three points. *Buildings.* 2026;16(1):188. https://doi.org/10.3390/buildings16010188

11. Liu L, Zhao S, Xin J, Wang Z. Simplified analysis of thermal cracks in low–heat Portland cement concrete. *Advances in Civil Engineering.* 2022;2022:7630568. https://doi.org/10.1155/2022/7630568 EDN: IQXPLS

12. Aniskin NA, Nguyen TC. Predictive model of temperature regimes of a concrete gravity dam during construction: Reducing cracking risks. *Buildings.* 2023;13(8):1954. https://doi.org/10.3390/buildings13081954 EDN: LFQTEG

13. Nguyen CT, Luu X.B. Reducing temperature difference in mass concrete by surface insulation. *Magazine of Civil Engineering.* 2019;4(88):70–79. https://doi.org/10.18720/MCE.88.7 EDN: HHFAQQ

14. Van Lam T, Nguen CC, Bulgakov BI, Anh PN. Composition calculation and cracking estimation of concrete at early ages. *Magazine of Civil Engineering.* 2018;82:13. https://doi.org/10.18720/MCE.82.13 EDN: YZNUZV

15. Van Tran M, La H, Nguyen T. Hybrid machine learning for predicting hydration heat in pipe-cooled mass concrete structures. *Construction and Building Materials.* 2025;481:141558. https://doi.org/10.1016/j.conbuildmat.2025.141558 EDN: OTLQKB

16. Sargam Y, Wang K, Cho I.H. Machine learning based prediction model for thermal conductivity of concrete. *Journal of Building Engineering.* 2021;34:101956. https://doi.org/10.1016/j.jobe.2020.101956 EDN: RIIOZE

17. Tuvayanond W, Kamchoom V, Prasittisopin L. Efficient machine learning for strength prediction of ready-mix concrete production (prolonged mixing). *Construction innovation.* 2026;26(2):369–394. https://doi.org/10.1108/CI-09-2023-0240 EDN: TEFJHH

18. Chou JS, Tsai CF, Pham AD, Lu YH. Machine learning in concrete strength simulations: Multi-nation data analytics. *Construction and Building materials.* 2014;73:771–780. https://doi.org/10.1016/j.conbuildmat.2014.09.054

19. Klemczak B, Bąba D, Siddique R. Machine Learning-Based Prediction of Heat Transfer and Hydration-Induced Temperature Rise in Mass Concrete. *Energies.* 2025;18(17):4673. https://doi.org/10.3390/en18174673 EDN: ZVWFTY

20. Do TA, Le BA. Machine learning approach for predicting early-age thermal cracking potential in concrete bridge piers. *Forces in Mechanics.* 2024;17:100297. https://doi.org/10.1016/j.finmec.2024.100297 EDN: STXYTP

21. Shahrokhishahraki M, Malekpour M, Mirvalad S, Faraone G. Machine learning predictions for optimal cement content in sustainable concrete constructions. *Journal of Building Engineering.* 2024;82:108160. https://doi.org/10.1016/j.jobe.2023.108160 EDN: THDUVM

22. Sun G, Du M, Shan B, Shi J, Qu Y. Ultra-high performance concrete design method based on machine learning model and steel slag powder. *Case Studies in Construction Materials*. 2022;17:e01682. https://doi.org/10.1016/j.cscm.2022.e01682 EDN: PNYATB

23. Forsdyke JC, Zviazhynski B, Lees JM, Conduit GJ. Probabilistic selection and design of concrete using machine learning. *Data-Centric Engineering*. 2023;4:e9. https://doi.org/10.1017/dce.2023.5 EDN: VLTCTA

24. Li Z, Yoon J, Zhang R, Rajabipour F, Srubar III WV, Dabo I, Radlińska A. Machine learning in concrete science: applications, challenges, and best practices. *npj Computational Materials*. 2022;8(1):127. https://doi.org/10.1038/s41524-022-00810-x EDN: BSEOLV

25. Nesvetaev GV, Koryanova YuI. Forecasting the strength gaining kinetics of the concrete hardening in the abnormal conditions. *Modern Trends in Construction, Urban and Territorial Planning*. 2023;2(4):59–68. (In Russ.) https://doi.org/10.23947/2949-1835-2023-2-4-59-68 EDN: UAIZPO

Несветаев Г.В., Корянова Ю.И. Прогноз кинетики прочности бетона при твердении в условиях, отличных от нормальных // Современные тенденции в строительстве, градостроительстве и планировке территорий. 2023. Т. 2. № 4. С. 59–68. https://doi.org/10.23947/2949-1835-2023-2-4-59-68 EDN: UAIZPO

26. Chepurnenko A, Nesvetaev G, Koryanova Y. Modeling non-stationary temperature fields when constructing mass cast-in-situ reinforced-concrete foundation slabs. *Architecture and Engineering*. 2022;7(2):66–78. https://doi.org/10.23968/2500-0055-2022-7-2-66-78 EDN: AKGXYN

27. Chepurnenko AS, Nesvetaev GV, Koryanova YI, Yazyev BM. Simplified model for determining the stressstrain state in massive monolithic foundation slabs during construction. *International Journal for Computational Civil and Structural Engineering*. 2022;18(3):126–136. https://doi.org/10.22337/2587-9618-2022-18-3-126-136 EDN: RQQYSK

28. Chepurnenko AS, Nesvetaev GV, Koryanova YuI, Shut VV, Tyurina VS. Experience of concreting a massive monolithic foundation slab. *Construction Materials and Products*. 2025;8(5):2. https://doi.org/10.58224/2618-7183-2025-8-5-2 EDN: ECAUPO

29. Chepurnenko A, Turina V. Simplified Method for Determining Thermal Stresses during the Construction of Massive Monolithic Foundation Slabs. *CivilEng*. 2023;4(3):740–752. https://doi.org/10.3390/civileng4030042 EDN: PBHJUB

30. Smolana A, Klemczak B, Azenha M, Schlicke D. Thermo-mechanical analysis of mass concrete foundation slabs at early age — essential aspects and experiences from the FE modelling. *Materials*. 2022;15(5):1815. https://doi.org/10.3390/ma15051815 EDN: SNFMFC